https://doi.org/10.1016/j.energy.2019.03.054

Performance Comparison of Two Flat-Plate Photovoltaic Thermal Collectors with Different Channel Configuration

Ying Yu[a,b], Hongxing Yang[b], Jinqing Peng[c], Enshen Long[a,*]

[a]*College of Architecture and Environment, Sichuan University, Chengdu 610065, China*
[b]*Renewable Energy Research Group (RERG), Department of Building Services Engineering, The Hong Kong Polytechnic University, Hong Kong, China*
[c]*College of Civil Engineering, Hunan University, Changsha 410082, China*

Abstract

A performance study with experiments and TRNSYS simulations was conducted for two water-type roll-bond photovoltaic /thermal (PV/T) collectors installed in Chengdu, western China. Two PV/T prototypes with different roll-bond absorber plates were designed and manufactured, one was made with the harp-channel configuration and the other one was produced with the grid-channel arrangement. Their performances were compared through experimental monitoring. The harp-channel PV/T collector had much lower pressure drop than that of the grid-channel PV/T collector. TRNSYS models for parallel-tube absorbers were seamlessly applied to the two roll-bond PV/T collectors with some input parameters altered or derived from experimental results. At the same time, the annual energy production of the two PVT- DHW (domestic hot water) systems were simulated and compared for three different cities of Sichuan Province. The results of the experiments and simulations demonstrated that the grid-channel PVT had higher thermal and PV efficiencies than that of the harp-channel collector. However, the system optimization is still needed to acquire an ideal solar fraction.

Keywords: Roll-bond absorber; Thermal efficiency; PV efficiency; Pressure drop; collector efficiency factor

1. Introduction

Photovoltaic thermal (PV/T) systems can supply electricity and thermal energy simultaneously. There are many different approaches for PV/T integration [1]. In a flat-plate water-type PV/T device, the thermal absorber is the key component which determines its performance. The different materials of absorber plates, different channels configuration and arrangement were introduced in the review paper by Aste [2]. In order to have better heat transfer property, metallic materials such as copper and aluminum were commonly used for making the absorber plate of PVT collectors. The typical channel configuration of the absorber plate was the sheet-and-tube type, which had two other variants: box channel and roll-bond types. However, their manufacturing techniques were totally different.

The sheet-and-tube absorber was the most widely used plate due to its easily producing and low cost merits [1, 3, 4]. Although the roll-bond technology has already frequently used in heat exchangers such as the evaporators of refrigeration, it was adopted in solar collectors [5, 6] and PVT applications in recent years [7]. The box channel (also called fully-wetted) absorber was commonly made by aluminum [8] and its fin efficiency was equal to 1, the maximum value of fin efficiency [9]. The performance comparison between the classical sheet-and-tube type and the box channel type under the same conditions showed that the box channel type had higher thermal and electrical efficiencies [10]. However, the manufacturing difficulty and the high cost limited the practical use of the box channel type on marketplace.

* Corresponding author. Tel.: +86-28- 85401015
E-mail address: Longes2@163.com

Nomenclature

A_c	area of the collector, normally gross area, m^2	U_L	overall heat loss coefficient from the absorber to the ambient, W/m^2·K
AM	air mass	U_t	top loss coefficient from the absorber to the ambient, W/m^2·K
C_p	specific heat capacity of water, kJ/kg·℃	v	wind velocity, m/s
D	tube or channels' outside diameter, m	V_{mpp}	voltage at maximum power point, V
D_h	hydraulic diameter of noncircular tube, m	W	distance between tubes or channels, m
F'	PVT collector efficiency factor	β	slope of the PVT collector surface
F_R	PVT collector heat removal factor	β_r	temperature coefficient of solar cell efficiency, %/℃
f_{sol}	solar fraction	δ	thickness, m
G_T	global solar irradiance on the module plane, W/m^2	ε_c	emissivity of the PV glass cover
h_{fj}	heat transfer coefficient between the fluid and the channel wall, W/m^2·K	η_e	electrical efficiency
h_v	wind convection coefficient, W/m^2·K	η_{th}	thermal efficiency
I_{mpp}	current at maximum power point, A	η_o	overall efficiency
$\dot{m}$	flow rate of fluid through the PVT collector, kg/s	η_{PES}	primary energy saving efficiency
Q_{AUX}	auxiliary heating rate, W	η_{power}	average efficiency of power plants at national level
Q_{DH}	domestic hot water load, W	σ	Stefan-Boltzmann constant, 5.67×10^{-8}W/m^2·K^4
W	electrical output of the module, W	χ	wetted perimeter, m
Q_e	overall thermal loss rate from the module, W	$(\tau\alpha)_{ef,}$	effective transmittance-absorptance product
Q_L	useful heat gain of fluid, W		
Q_u	effective absorbed solar radiation for absorber plate, W/m^2	**Subscript**	
S	ambient temperature, ℃	1	refers to the parameters of PVT 1
T_a	inlet fluid temperature, ℃	2	refers to the parameters of PVT 2
T_{fi}	outlet fluid temperature, ℃	PV	refers to the parameters of photovoltaic cells
T_{fo}	mean fluid temperature, ℃	T	refers to the parameters on a tilted plane
T_{fm}	reduced temperature, ℃·m^2/W	ref	refers to the reference conditions (i.e. G_T = 1000W/m^2, T_{PV}=25℃, AM=1.5)
T_r	overall heat transfer coefficient from the absorber to the fluid, W/m^2·K		
U_f			

The study on thermal collectors with roll-bond absorbers was firstly reported in 2011 [6]. Del Col et al. [11] had studied different solar collectors and revealed that the higher thermal performance achieved by the roll-bond collector was due to the more channels in the absorber. Furthermore, a roll-bond absorber was made of two aluminum sheets rolled together, with liquid channels formed by inflating air at high pressure [11]. Thus, a roll-bond absorber has the liquid channels integrated with the absorber plate. In addition, the channels could be designed in different configurations according to the purpose. By far, many studies on the electrical and thermal performance of different PVT types have been carried out with experimental and simulation methods [10, 12-14], but only a few cases focused on roll-bond PVT collectors [7, 15]. The comparison between the classical sheet-and-tube and the roll-bond design was more challenging due to the very different geometric characteristics of the channels in roll-bond absorbers.

As a simulation tool for renewable energy systems, TRNSYS had been used to model and simulate PVT systems [3, 16] in some cases. The numerical models of PVT in TRNSYS were for traditional sheet-and-tube absorber based on Florschuetz's PVT model, adapted from the steady-state model of flat-plate collectors [17], and suitable for predicting the performance of the PVT integrated with the parallel-channel absorber. However, for roll-bond PVT collectors, the channels were not circular and mostly non-parallel. So far, few studies have been done to examine the software's applicability for roll-bond PVT collectors.

In this paper, two PVT collectors with different roll-bond absorber plates were designed and manufactured. One was with harp-channel configuration and the other one was with the grid-channel

arrangement, shown in Figure 1 and Figure 2, respectively. Their thermal performance and electrical property were compared experimentally under the climatic condition of western China. A new bonding technique was applied to connect the PV laminate and the absorber plate. TRNSYS models for parallel-tube absorbers were applied to these two roll-bond absorbers with some input parameters being altered. At the same time, the annual energy production of the two PVT- DHW systems was simulated and compared.

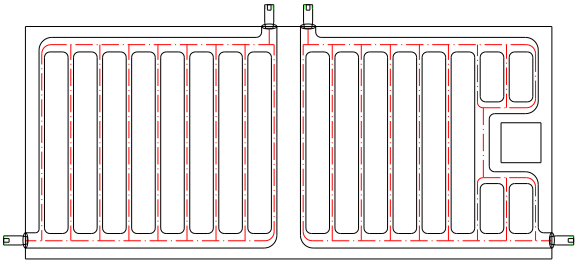

Figure 1 Harp-channel absorber plate

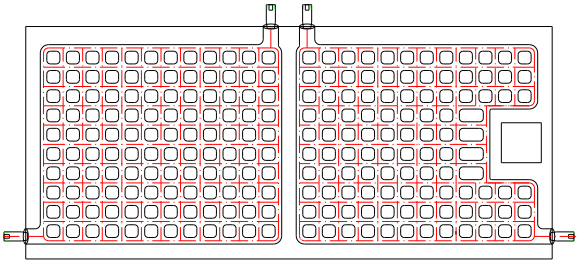

Figure 2 Grid-channel absorber plate

2. System Design and description

The PVT system was ultimately applied to providing domestic hot water (DHW) and partial electricity to rural households or shelters, so the cost should be considered in the first place for system design.

Two prototypes of PVT-DHW systems were made and the study focused on the performance of two PVT collectors, only different in the absorber. Both thermal absorber plates were roll-bond aluminum plates, each size of 1450×640×1.5mm. Hereinafter the harp-channel absorber is called Absorber 1 and the grid-channel one is called Absorber 2. Likewise, the hybrid collector with Absorber 1 is PVT 1, with Absorber 2 is PVT 2. Besides the different channel configuration of the absorber, the two test rigs had the same composition with the unglazed PVT modules, the water tank, as well as some control valves and check valves, connected with polypropylene-random (PP-R) pipe as an open natural-circulation loop system, meanwhile, a standby pump was connected in parallel as the bypass of the loop and worked as needed. Figure 3 shows the schematic diagram of the test rig 2 with the grid-channel absorber in the hybrid collector.

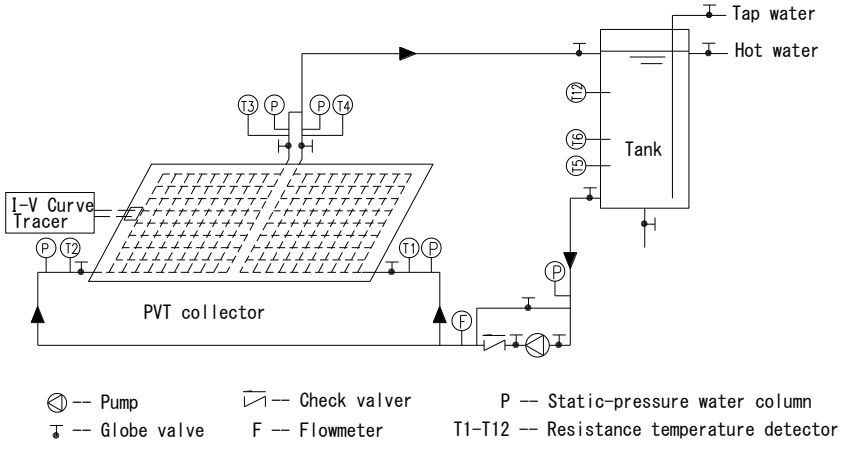

Figure 3 Schematic diagram of the PVT test rig 2

The semi-finished commercial PV panels were adopted in view of cost control and easy availability. Each was of size 1480×670×5mm, comprised of 36 poly-crystalline (mc-Si) solar cells, having an efficiency of 15.43% at STC and a power temperature coefficient of 0.44%/℃. Both hybrid collectors were insulated by 40mm rubber plastic foam at the back side of the absorber plates. The specifications and design

parameters of the components are summarized in Table 1. The values came from test data, manufacturer's manual, or relevant literature.

Table 1. Specifications of the PV lamination and parameters of the thermal absorbers

Parameter	Value	
PV laminate	1480×670×5 mm	
Maximum power (STC)	153.04 W_P	
Maximum voltage	18.03 V	
Maximum current	8.80 A	
Open circuit voltage	22.45 V	
Short circuit current	9.34 A	
Temperature coefficient of solar cell efficiency	-0.44 %/℃	
Absorber plate 1450×640×1.5mm	***Absorber 1***	***Absorber 2***
Number of channels	18	-
Channel distance	80 mm	-
Channel length	600 mm	-
Channel width	15mm	18mm
Cross section area of a channel	19.7 mm^2	26.7 mm^2
Hydraulic diameter of the channel (noncircular)	3.24 mm	3.28 mm
Area ratio of the channel to plate	0.26	0.49
Water volume	1.96 L	2.30 L
Thermal insulation		
Thickness of back insulation	0.04 m	
Thickness of frame insulation	0.02 m	
Conductivity	0.036 W/m·K	

The PV-absorber bonding method was inspired by the package lamination method [2]. A layer of ethylene-vinyl acetate (EVA) was used as the adhesive. Each PV panel was thermo-laminated on a roll-bond absorber plate through EVA adhesive under high pressure and temperature which was similar to the process of combining solar cells with a TPT (Polyester/ Tedlar tri-laminate) back sheet. Thus, in our PVT collector, the bonding structure consists of EVA, TPT, EVA three layers, producing a theoretical heat transfer coefficient of 219 $W/m^2 \cdot K$ between PV cells and the absorber, which is about twice more than the measured value of 100 $W/m^2 \cdot K$ by means of gluing bonding reported by Van et al [18].

3. Methodology

3.1. Simulation

To compare the annual outputs of the two PVT collectors, dynamic simulations were conducted for the two systems. The modified Hottel-Whillier-Bliss model was adopted to theoretically evaluate the performance of PVT collectors, which relied on Florschuetz's [17] work stemming from the model for solar thermal collectors [19]. It is suitable for all absorber plates with parallel tubes (or risers), e.g. sheet-and-tube absorbers. In this model, the absorber plate section between two adjacent parallel tubes is regarded as the straight fin, which is a classical fin-tube heat transfer problem. With the similar assumption set in the Hottel-Whillier-Bliss model, the differential equation of steady-state energy balance for a PVT collector was established. Finally, the thermal output of PVT is decided by its operating condition and some

attribution parameters such as the overall heat loss coefficient U_L, the collector efficiency factor F' or the heat removal factor F_R. The useful heat gain of the PVT collector is calculated by:

$$Q_u = A_c F' \left[G_T (\tau\alpha)_{\text{eff}} (1 - \eta_e) - U_L (T_{fm} - T_a) \right] \quad (1)$$

$$\eta_{th} = \frac{Q_u}{G_T A_c} \quad (2)$$

In Equation (1), the collector efficiency factor F' can be calculated by the standard fin efficiency F, which is a hyperbolic tangent function of absorber geometric parameters such as the tube diameter D, and the tube spacing W. The F' of a conventional sheet-and-tube PVT is calculated by this approach. Differently, for PVT 1 with the harp-channel absorber, the wetted perimeter of channel χ was adopted instead of the tube perimeter πD in the expression of F' as follow:

$$F' = \frac{1}{\frac{W}{D + (W - D)F} + \frac{W U_L}{\chi h_{fi}}} \quad (3)$$

where D was not the diameter but the open width of a noncircular channel.

PVT 2 with grid-channel could not directly be analysed by the model until its parameter F' being deduced from experimental data.

For more directly interpretation, the reduced temperature is introduced as:

$$T_r = \frac{T_{fm} - T_a}{G_T} \quad (4)$$

where T_{fm} is the mean water temperature and T_a is the ambient temperature. The thermal efficiency is conventionally expressed as a function of T_r, and equation (4) can be given as a linear expression:

$$\eta_{th} = F' [(\tau\alpha)_e (1 - \eta_e) - U_L T_r] = \eta_{t0} - a_1 T_r \quad (5)$$

where η_{t0} is the thermal efficiency at zero reduced temperature and $a_1 = -F' U_L$ relates to the heat loss coefficient of PVT collectors.

The overall heat loss of the PVT collectors consisted of the external radiative and convective heat loss from the top and back of the panel to the sky and ambient. The effective sky temperature T_{sky} was used to account for long-wave radiation losses from the top surface to the sky. It was usually assumed equal to the ambient temperature T_a because the difference made by the assumption can be neglected in evaluating heat gain performance [19]. Another assumption was that the temperature of the glass cover was equal to T_{PV}. Therefore, the heat loss coefficients of the PVT collector were calculated as follow:

$$U_L = U_t + U_b + U_e \quad (6)$$

$$U_t = h_v + \sigma \varepsilon_c (T_{PV}^2 + T_a^2)(T_{PV} + T_a) \quad (7)$$

$$h_v = 2.8 + 3.0v \quad (8)$$

where U_b, U_e are the bottom and the edge loss coefficients, respectively [19].

This model together with the altered attribution parameter was applied to simulate the performance of the PVT module with the roll-bond absorber, implemented in the software TRNSYS. Specifically, the calibrated Type50 model was adopted because its simulated results had good agreement with the experimental data from the previous study [20].

The PV cells were assumed to be operating at their maximum power point. According to the test results of Evans et al. [21], the cell efficiency can be regarded as a linearly decreasing function of the absorber temperature over its operating temperature range. Based on parameters under Standard Test Conditions and the power temperature coefficient of solar cells β_r, the real PV efficiency is given by:

$$\eta_e = \eta_{\mathrm{ref}}[1 - \beta_r(T - T_{\mathrm{ref}})] \tag{9}$$

The other factors affecting the actual PV efficiency include the angle of incidence, the solar spectrum, and low irradiance. Mostly, they are neglected and the temperature factor is only taken into account.

The overall efficiency of the PVT is simply defined as the total amount of thermal and electrical efficiency:

$$\eta_o = \eta_{th} + \eta_e \tag{10}$$

or in terms of primary energy, it can be defined as:

$$\eta_{PES} = \eta_{th} + \frac{\eta_e}{\eta_{power}} \tag{11}$$

In China, the average convert efficiency of power plants is 0.38.

On the other hand, the performance of a PVT-DHW system is not only determined by the quality of the hybrid collector, but also evaluated by the solar fraction f_{sol}, which is the ratio of solar heat gain of the system to the total thermal energy demand or load. The rest un-covered thermal demand should be met by auxiliary energy Q_{AUX}. For a PVT-DHW system, the solar fraction is calculated as:

$$f_{sol} = 1 - \frac{Q_{AUX}}{Q_{DHW}} \tag{12}$$

The domestic hot water load Q_{DHW} is equal to the sum of Q_u and Q_{AUX} minus the heat loss of the tank and the possible electrical energy for the system running.

Generally, the solar fraction of a PVT system is not as high as a pure solar thermal system because a part of received solar energy has to transfer to electrical energy. Besides, a hybrid collector should be avoided overheating in summer, thus, the optimal f_{sol} is between 0.4-0.6 [2].

3.2. Experiments

Experiment on two PVT test-rigs was conducted on the roof of a residential building in the city Chengdu. The stagnation temperature, the critical radiation level, the pressure drop of the absorbers were monitored. When the weather condition met the steady-state conditions of the EN12975 standard for outdoor tests [22], the steady-state thermal performance of the PVT collectors could be obtained. Otherwise, transient efficiencies under different conditions could be acquired.

The monitoring sensors and devices were connected to the test rig, as shown in Figure 3, consisting of the following items in two test rigs:

- two EKO MS-802 pyranometers for horizontal and tilt global solar irradiation respectively, one JTTS-04 pyranometer for horizontal diffuse irradiation;
- an EKO MP-160 I-V Checker for monitoring two PVT modules in turn;
- two turbine flowrate sensors in each main loop;

- sixteen Pt100 resistance temperature detectors located in inlets and outlets of the PVT water loop, or immersed in water tank equidistantly in the depth direction;
- nine water columns connected in different positions of the water loop for measuring the pressure drop in the related segment;
- a JTSOFT-3.0 for measuring wind speed and ambient temperature and humidity near the PVT collector;
- data acquisition system: GL800 Data Logger, TH-TZ16.

Sometimes, an infrared camera Fluke TiX560 was used to observe the temperature distribution on the PVT surface.

Most experimental data were recorded at one-minute interval, apart from the electricity data. The I-V curve Tracer was used to monitor every PV module every minute in turn, so for each module the recording time step was 2 minutes.

With the measurement of water temperatures at the inlet and outlet of the PVT collector, the flow rate, and the incidence solar irradiance, as well as V_{mpp} and I_{mpp}, the checked voltage and electric current at the maximum power point (MPP) operation, the thermal and electrical performance of the test module can be given by:

$$\eta_{th} = \frac{\dot{m}C_p\left(T_{fo} - T_{fi}\right)}{G_T A_c} \tag{13}$$

$$\eta_e = \frac{V_{mpp} I_{mpp}}{G_T A_c} \tag{14}$$

4. Results and discussion

4.1. Pressure drop

For the purpose of simplifying the PVT system, the feasibility research on the natural circulation mode was carried out by measuring the pressure drops of the two roll-bond absorbers at different flow rates. The pressure drop of an absorber is the main share of the hydraulic resistance in a PVT liquid loop and the latter determines the liquid circulation mode in the PVT collector. In this research, each absorber was designed with two symmetrical water loops (see Figure 1 and 2) in order to reduce the whole pressure drop of the absorber.

Figure 4 gives the comparison of pressure drops in the two absorbers. It can be found that the pressure drop of Absorber 1 is close to linear growth from 100 Pa (at 0.1 L/min·m^2) to 400 Pa (at 2.0 L/min·m^2), but of Absorber 2 has a quadratic exponential growth with the flow rate increased. For instance, 747 Pa of Absorber 2 corresponds to 225 Pa of Absorber 1 at the common flow rate of 1.2 L/min·m^2. Correspondingly, the rest pressure drop of the water loop was under 100 Pa, caused by valves and pipe hydraulic resistance.

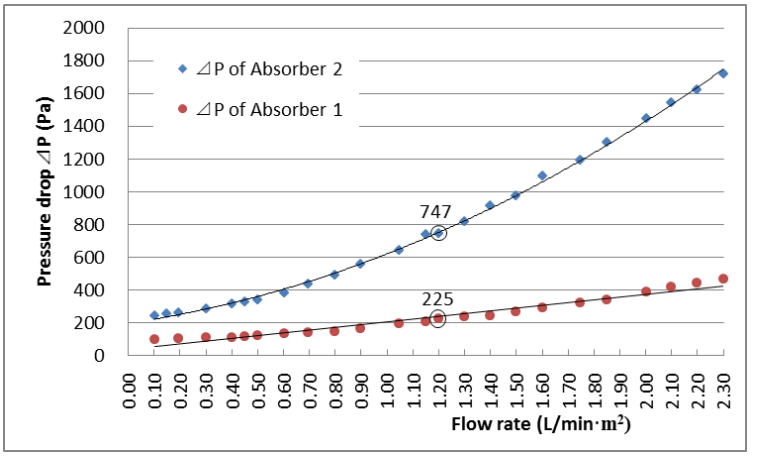

Figure 4 Pressure drops of the two absorbers

In the earliest test, when the water tank was set above the PVT collectors of 1.2 m, the natural circulation was observed with a very small flow rate under 0.2L/min·m^2 in two systems, and a notable temperature difference above 20℃, shown in Figure 5, which had adverse effect on conversion efficiency of PV cells.

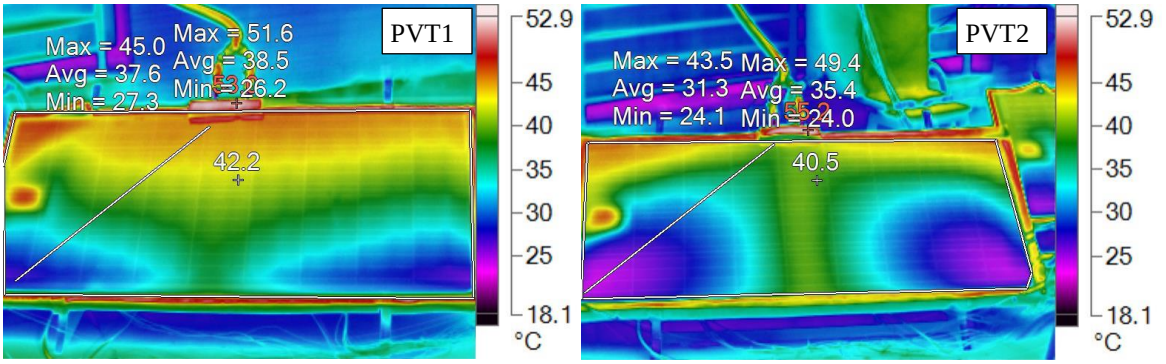

Figure 5 Temperature images of the two PVT surfaces under natural circulation (12:07 PM , 6/16/2017)

On the test moment (12:07 PM on 6/16/2017) the ambient temperature was 27 ℃. And the stagnation temperature of that day, recorded at 11:47 AM, was about 57 ℃ in both PVT collectors.

According to the pressure drop feature of the PVT 1 collector, if the central-point height difference between the water tank and the PVT panel increases to 4 m, the flowrate of 0.5 L/min·m^2 would be obtained by gravity circulation with a water temperature difference about 10℃. The case is applicable to low-rise housing in rural areas with abundant space in front of the house. Otherwise, the mechanical circulation has to be adopted without such conditions. But for PVT 2 system, the water tank must be placed at 10 m higher than the PVT collector so as to produce the same natural-circulation flow rate and the same water temperature difference, which may not be the practical situation. So for most time of the experiment, mechanical circulation was adopted and the temperature differences between the inlet and the outlet of either PVT collector were usually controlled within 5 ℃ and the utmost no more than 10℃. The flow rate was adjusted between 0.6 – 1.5 L/min·m^2.

4.2. Thermal and electrical efficiency

The daily performance monitoring was carried out under the typical local weather condition from June of 2017 to May of 2018. Figure 6, 7 depicts the transient efficiencies of the two PVT systems on a clear day and a cloudy day respectively.

On April 16th, 2018, the average thermal efficiencies of PVT 1 and PVT 2 were 27.5% and 28.9% respectively, which suggests the grid-channel absorber had better thermal performance. The average PV efficiencies of PVT 1 and PVT 2 were 11.2% and 11.6% respectively, the latter was higher than the former.

On Sept. 20th, 2017, the average thermal efficiencies of PVT 1 and PVT 2 were 24.6% and 26.6% respectively, and the average PV efficiencies of PVT 1 and PVT 2 were 10.6% and 11.1% respectively, which suggests the same feature of the comparative result.

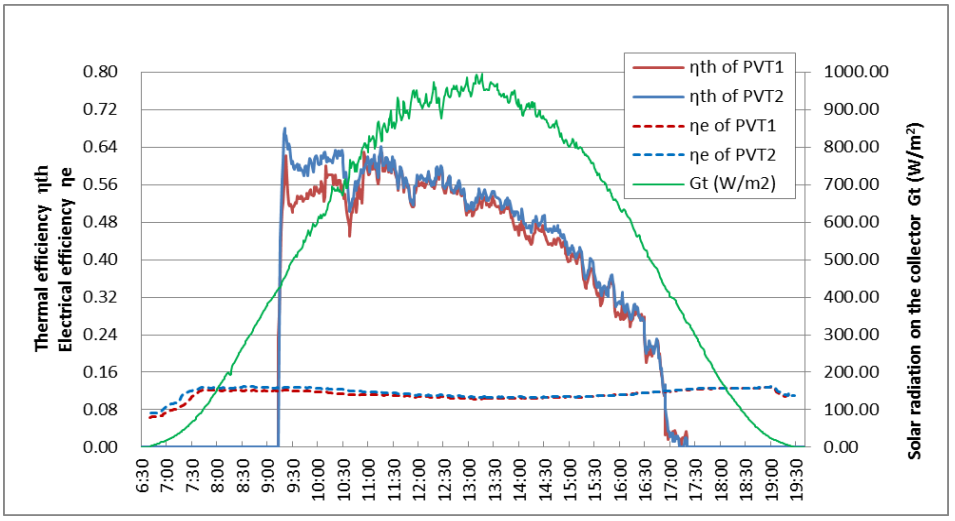

Figure 6 Thermal and PV efficiencies of two PVT collectors on a clear day (4/16/2018)

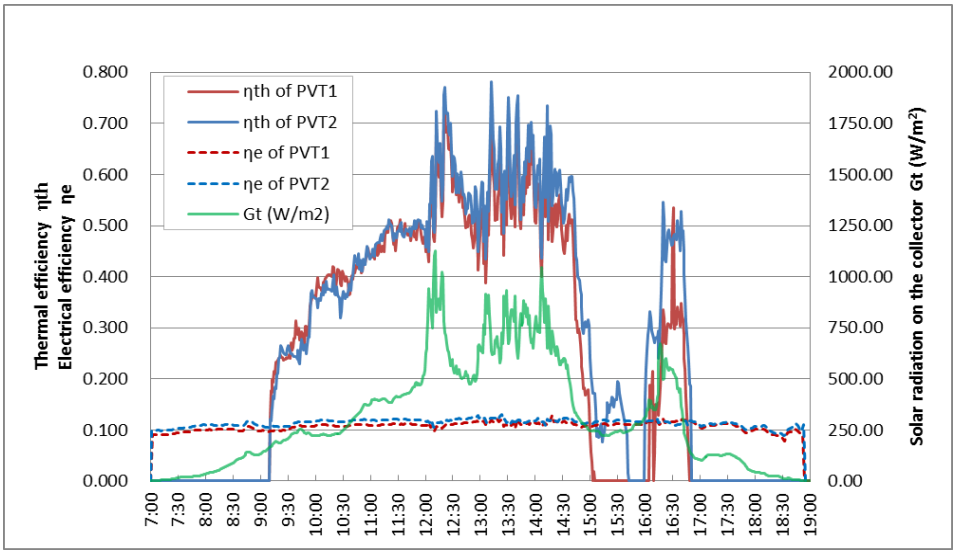

Figure 7 Thermal and PV efficiencies of two PVT collectors on a cloudy day (9/20/2017)

The data indicate that either thermal or electrical performance of PVT 2 with the grid-channel absorber is generally superior to that of PVT 1 with the harp-channel absorber. Because the higher thermal efficiency, the more heat can be removed, the lower PV cell temperature is obtained, therefore the better photoelectric conversion efficiency is realized.

During the experiment period, only 4 days' weather condition could meet the steady-state test demand according to thermal performance test standards. Figure 8 shows the transient thermal efficiencies of the test around solar noon on March 22th, 2018 with solar radiation ranging from 880 to 940 W/m^2. The ambient temperature was 22.6±1.0℃ and wind speed varied between 2.2-3.0 m/s. The inlet water temperatures of both PVT systems were controlled within 30-45℃, with the flow rates of 1.2 kg/min·m^2.

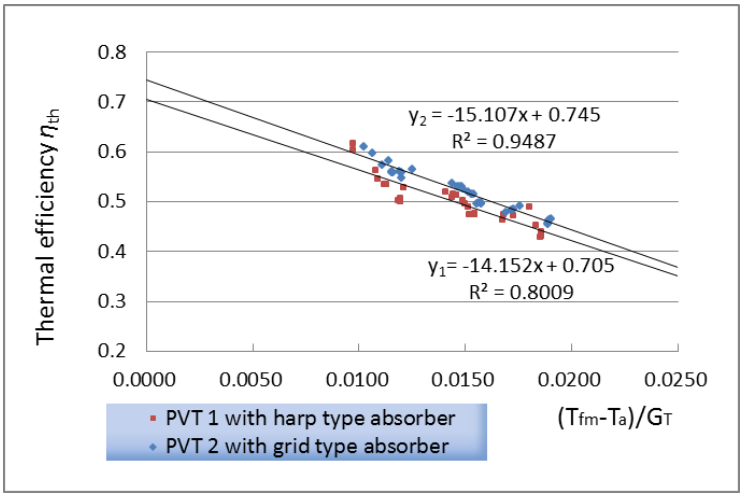

Figure 8 Comparison of standard thermal efficiencies of two PVT collectors

The test data were plotted as thermal efficiency versus the reduced temperature $(T_{fm}- T_a)/G_T$, and T_{fm} is the arithmetic average of inlet and outlet water temperatures. In Figure 8, The intercepts of two trend lines are 70.5% and 74.5% representing the thermal efficiencies of PVT 1 and PVT 2 respectively at zero reduced temperature, occurred when the average water temperature equals to the ambient temperature, indicating the good thermal performance of this two PVT modules and their comparative result aligned with the aforementioned results.

The slopes of the two trend lines are 14.2 and 15.1 representing the heat loss characteristics of PVT 1 and PVT 2 respectively, and equal to their $(F'U_L)$ according to Equation (5). The collector efficiency F' is a function of U_L and h_{fi}, and each of which is weak temperature dependence [19]. For Absorber 1, the heat transfer coefficient between the fluid and the channel wall h_{fi} was calculated about at 800 W/m^2·K when the flow rate is 1.2 kg/min·m^2. The overall heat loss coefficient U_L is strongly affected by wind speed. The annual wind speed in Sichuan Basin is usually low. Though some meteorological data [23] suggests average hourly wind speed may reach 3-5 m/s in Chengdu, our measured mean minute wind speed on experimental site mostly ranged from 0-2m/s, in particular, mean wind speed in majority of daytime fell below 1 m/s. Hence, the U_L for two PVT collectors in this experiment ranged from 12-16.5 W/m^2·K when the temperature of the PV cells fell within 20-45 ℃ and the ambient temperature fell within 5-35 ℃, which covered the most of the operating conditions. With these elementary data and the geometrical structural parameters in Table 1, the collector efficiency F' for PVT 1 could be determined as 0.92. So, the average U_L was calculated as 15.5 W/m^2·K for this PVT 1 collector on the test day.

With regard to PVT 2, it was not so smooth for this approach to deduce its F', for the channel arrangement was not parallel. But for these two hybrid collectors, the influential factors of U_L were same

except for differences in fluid temperature, normally $\leqslant 2$℃. Since U_L is not sensitive to temperature, the small temperature difference between two PVT panels was neglected, the average U_L of PVT 2 collector on the test day could be regarded as the same as that of PVT 1. Therefore, the collector efficiency F' for PVT 2 could be estimated to 0.97 according to the slope of the trend line of PVT 2 in Figure 8.

4.3. Simulation results

With the parameters F' known, the performance simulation for both PVT systems could be carried out by the tool TRNSYS.

The PVT-DHW system applied in rural families was designed with following conditions: A family of 4 persons; a stratified water tank of 220 L with an auxiliary heater of 1500 W; 3.96 m^2 PVT collector (equivalent of 4 pieces of the prototype). The daily water consumption 50 L/person at 60℃ was according to the Chinese standard [24] and the consumption profile, shown in Figure 9, coming from the living habit of Chinese rural area. The pump was controlled by a differential controller according to the difference between PVT outlet water temperature T_{fo} and the temperature of water from the tank to PVT. The annual output of such a PVT-DHW system could be dynamically simulated in TRNSYS.

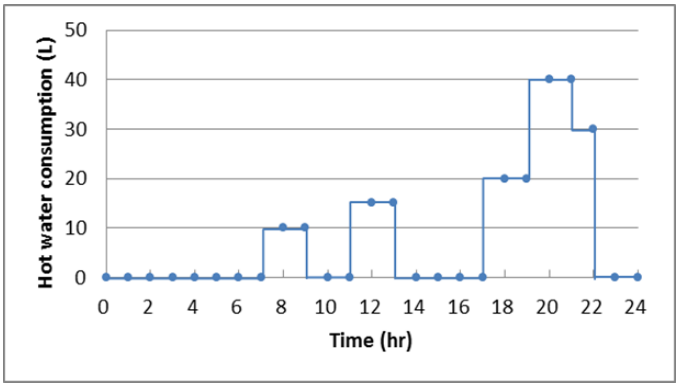

Figure 9 Comparison of standard thermal efficiencies of two PVT collectors

Two PVT-DHW systems, with the harp-channel absorber and the grid-channel absorber respectively, were compared by simulating their yearly energy production. Apart from the same design conditions and same hot water consumption, two PVT collectors had identical slopes of 33° and azimuth angles of 0°. In order to compare the PVT performance in different cities, the more comprehensive, hourly-based meteorological data available from EnergyPlus were adopted to input to TRNSYS for simulation. Table 2 shows the yearly overall efficiencies of two PVT-DHW systems in Chengdu. Their overall efficiency and primary energy saving efficiency were calculated.

Table 2 Yearly overall performance comparison of two PVT-DHW systems in Chengdu

Parameter	PVT(1)-DHW (harp-channel absorber)	PVT(2)-DHW (grid-channel absorber)
Q_e (kWh/year)	406.03	406.94
η_e	11.8%	11.8%
Q_u (kWh/year)	836.29	869.57
η_{th}	24.2%	25.2%
η_o	36%	37%

η_{PES}	55.3%	56.3%
Q_{AUX} (kWh/year)	1925.35	1895.05
Q_{DHW} (kWh/year)	2554.59	2554.29
F_{sol}	0.296	0.318

From Table 2, the system 2 with grid-channel absorber is still superior to system 1, although the advantage is not obvious. The influential factors to the whole PVT-DHW system are more complex, so the only difference in absorber carried little weight.

Chengdu (N 30.67°, E 104.02°) is located in central Sichuan Basin, where solar irradiance was weak compared with most regions in China. Nevertheless, the yearly efficiencies in Table 2 are not bad, only the solar fraction is below the low limit of the optimal value given by Aste et al. [2], and it can be increased by optimizing the storage tank, or increasing the collector areas directly.

Then, considering other two cities Mianyang (N 31.45°, E 104.73°) and Xichang (N 27.90°, E 102.27) in Sichuan Province, the annual outputs and efficiencies of the same PVT-DHW system located in three cities of Sichuan Province are shown in Figure 10. Their overall electrical efficiencies were almost the same, and overall thermal efficiency gaps were just 1% respectively. However, Xichang, Located in the margin of the basin, has obvious higher energy outputs and the solar fraction than those of the other two cities. The total tilted surface insolation for a typical year is 869.50 kWh/m^2 in Chengdu, 972.96 kWh/m^2 in Mianyang, and 1363.75 kWh/m^2 in Xichang, indicating that the decisive factor of the PVT-DHW performance is still the annual solar irradiance.

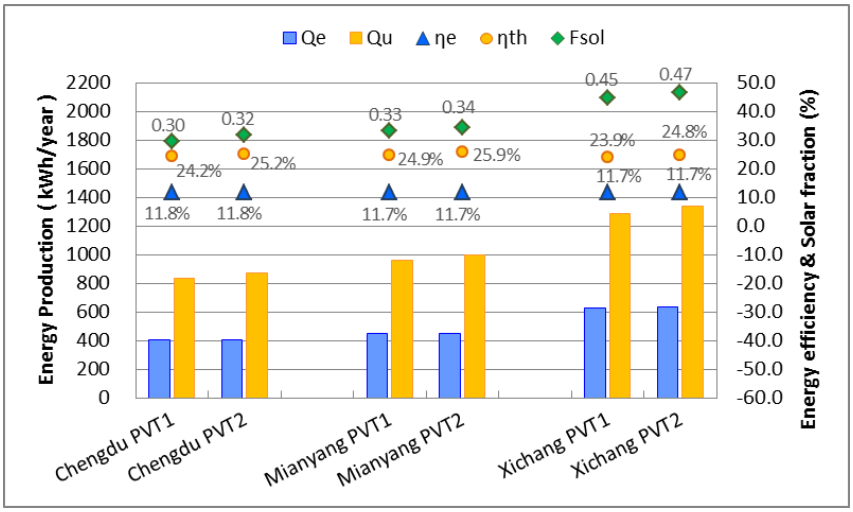

Figure 10 Comparison of outputs and efficiencies of two PVT systems

5. Conclusions

This paper presents a comparative study on two water-type flat-plate PVT collectors through experimental and simulating methods. The two hybrid collectors only differed in absorber channels, one was traditional parallel arrangement called harp-channel, and the other one was grid-channel. The manufacturing costs for these two configurations of absorber are nearly equal due to the roll-bond manufacture technique.

A performance monitoring was conducted on the two PVT prototypes in Chengdu, Sichuan Basin under the typical local weather condition from June of 2017 to May of 2018. The test results demonstrated that

the thermal and electrical efficiencies of the PVT 2 were generally higher than that of PVT 1, no matter on clear days or cloudy days. However, the advantage of PVT 2 was not obvious, especially in electrical output. Moreover, the difference was further reduced in terms of the annual simulated performance on the whole PVT-DHW system. Nevertheless, the thermal efficiencies at zero reduced temperature reached 70.5% for PVT 1 and 74.5% for PVT 2, indicating the good thermal performance of the two roll-bond PVT collectors, which can be interpreted as the result of low heat resistance of the PV-absorber connection, and the more channels of Absorber 2 than that of Absorber 1.

On the other hand, the Absorber 1 had a much lower pressure drop compared with the Absorber 2. At common flow rate ranging from 0.6 to 1.5 L/min·m^2, the pressure drop of the Absorber 1 was 1/3 to 1/2 of the pressure drop of Absorber 2, which made it possible for PVT 1 to work under a natural circulation mode at a low flow rate, or use less electricity under a mechanical circulation mode. In addition, PVT 1 had lower thermal inertia due to the lower water volume in Absorber 1, 1.96 L vs 2.30 L in Absorber 2. So each PVT collector has its own merit. Efforts still should be made in channel configuration optimization.

For the harp-channel roll-bond absorber, the evaluation method of collector efficiency factor *F'* was similar to that of the common sheet-and-tube absorber, but for the non-parallel channel absorber, the factor *F'* can be obtained through the standard performance test. Then, the performance of both PVT systems could be simulated smoothly by TRNSYS. The results of the annual energy simulation suggested that both PVT-DHW systems had almost the same overall efficiencies and primary energy saving efficiency. However, the system should be optimized in storage tank volume, collector area, and slope of the collector plane to achieve an ideal solar fraction in the area where solar energy is not so abundant.

Acknowledgments

The author would like to express appreciation to Hong Kong Jockey Club for providing financial support for the joint PhD program, and also the Department of Building Services Engineering, The Hong Kong Polytechnic University for providing testing devices and software support for this study.

References

[1] Chow T T. A review on photovoltaic/thermal hybrid solar technology. Appl Energ. 2010;87:365-79.
[2] Aste N, del Pero C, Leonforte F. Water flat plate PV–thermal collectors: A review. Solar Energy. 2014;102:98-115.
[3] Nualboonrueng T, Tuenpusa P, Ueda Y, Akisawa A. The performance of PV‐t systems for residential application in Bangkok. Progress in Photovoltaics: Research and Applications. 2012;21:1204-13.
[4] He W, Zhang Y, Ji J. Comparative experiment study on photovoltaic and thermal solar system under natural circulation of water. Applied Thermal Engineering. 2011;31:3369-76.
[5] Hermann M. Develop of a Bionic solar collector with alluminium roll-bond absorber. 2011.
[6] Del Col D, Dai Prè M, Bortolato M, Padovan A. Experimental characterization of thermal performance of flat plate solar collectors with roll-bond absorbers2011.
[7] Dupeyrat P, Ménézo C, Rommel M, Henning H-M. Efficient single glazed flat plate photovoltaic–thermal hybrid collector for domestic hot water system. Solar Energy. 2011;85:1457-68.
[8] Shan F, Tang F, Cao L, Fang G. Performance evaluations and applications of photovoltaic–thermal collectors and systems. Renewable and Sustainable Energy Reviews. 2014;33:467-83.
[9] Kim J-H, Kim J-T. The Experimental Performance of an Unglazed PV-thermal Collector with a Fully Wetted Absorber. Energy Procedia. 2012;30:144-51.
[10] Kim J-H, Kim J-T. The experimental performance of an unglazed PVT collector with two different absorber types. International Journal of Photoenergy. 2012;2012.
[11] Del Col D, Padovan A, Bortolato M, Dai Prè M, Zambolin E. Thermal performance of flat plate solar collectors with sheet-and-tube and roll-bond absorbers. Energy. 2013;58:258-69.
[12] Zondag HA, de Vries DW, van Helden WGJ, van Zolingen RJC, van Steenhoven AA. The yield of different

combined PV-thermal collector designs. Solar Energy. 2003;74:253-69.
[13] Zondag HA, de Vries DW, van Helden WGJ, van Zolingen RJC, van Steenhoven AA. The thermal and electrical yield of a PV-thermal collector. Solar Energy. 2002;72:113-28.
[14] Chow TT. Performance analysis of photovoltaic-thermal collector by explicit dynamic model. Solar Energy. 2003;75:143-52.
[15] Aste N, Del Pero C, Leonforte F. Thermal-electrical Optimization of the Configuration a Liquid PVT Collector. Energy Procedia. 2012;30:1-7.
[16] Haurant P, Ménézo C, Gaillard L, Dupeyrat P. A Numerical Model of a Solar Domestic Hot Water System Integrating Hybrid Photovoltaic/Thermal Collectors. Energy Procedia. 2015;78:1991-7.
[17] Florschuetz L. Extension of the Hottel-Whillier model to the analysis of combined photovoltaic/thermal flat plate collectors. Solar energy. 1979;22:361-6.
[18] van Helden WGJ, van Zolingen RJC, Zondag HA. PV thermal systems: PV panels supplying renewable electricity and heat. Progress in Photovoltaics: Research and Applications. 2004;12:415-26.
[19] Duffie JA, Beckman WA. Solar engineering of thermal processes. 4th ed: Wiley New York etc.; 2013.
[20] Yu Y, Long E, Chen X, Yang H. Performance Study on an Unglazed Photovoltaic Thermal Collector Running in Sichuan Basin. ICAE 2018. Hong Kong2018.
[21] Evans DL, Facinelli WA, Otterbein RT. Combined photovoltaic/thermal system studies. Arizona State Univ., Tempe (USA). Dept. of Mechanical Engineering; 1978.
[22] EuropeanStandard. EN 12975-2:2006 Thermal solar systems and components-Solar collectors-. Part 2: Test methods2006.
[23] 张晴原, 杨洪兴. 建筑用标准气象数据手册. 北京: 中国建筑工业出版社; 2012.
[24] National standards of the People's Republic of China: Code for design of building water supply and drainage. GB 50015-2003. Beijing: China planning press; 2010.